ORNL/TM-2018/1062
CRADA/NFE-17-06446

Development of mathematical model and simulation tool for the high capacity production of carbon fiber

CRADA Final Report
for
CRADA Number NFE-17-06446

Approved for Public Release.
Distribution is unlimited.

Srikanth Allu (ORNL)
Srdjan Simunovic (ORNL)
Tae-Seok Lee (Harper Intl)
Peter Witting (Harper Intl)

February 2019

OAK RIDGE NATIONAL LABORATORY
MANAGED BY UT-BATTELLE FOR THE US DEPARTMENT OF ENERGY

ORNL/TM-2018/1062
CRADA/NFE-17-06446

High Performance Computing for Manufacturing Final Report

Development of mathematical model and simulation tool for the high capacity production of carbon fiber

Srikanth Allu, Srdjan Simunovic (ORNL)
Tae-Seok Lee, Peter Witting (Harper International)

Date Published: February 2019

Prepared by
OAK RIDGE NATIONAL LABORATORY
Oak Ridge, Tennessee 37831-6283
managed by
UT-BATTELLE, LLC
for the
US DEPARTMENT OF ENERGY
under contract DE-AC05-00OR22725

Table of Contents

1. INTRODUCTION 3

2. PROBLEM DESCRIPTION 5

3. IMPACT 6

4. MODELLING APPROACH 6

5. MODEL DEVELOPMENT AND SIMULATIONS 9

5.1 3D COMPRESSIBLE FLOW MODEL 9
5.2 CHEMICAL COMPOSITION OF OFF-GAS AND 1D FIBER CONVERSION MODELING 11
5.3 CFTF LOW TEMPERATURE FURNACE MODEL 18

6. CONCLUSIONS AND FUTURE WORK 21

7. ACKNOWLEDGEMENTS 22

8. REFERENCES 22

9. APPENDIX 23

Executive Summary:

Weight reduction in the transportation is the most effective way for reducing fuel consumption. Carbon fiber composites have been increasingly used by automotive manufacturers in vehicle non-structural and structural parts. Larger penetration of carbon fiber-based materials requires very large quantities of fiber at a low price, and of consistently high quality. The advancements in carbon fiber technology that are required to achieve this production scale-up and cost reduction, are very challenging. The most expensive production step is the conversion of textile-grade polyacrylonitrile (PAN) precursor to carbon fiber. The conversion takes place in three main stages: stabilization, low and high temperature carbonization. Most of the research to date has focused on the stabilization of the PAN precursors and oxidized PAN fibers. Comparingly little effort has been dedicated to the investigation of processing conditions during low temperature (LT) carbonization. During this stage of fiber conversion, the largest fiber mass loss occurs, and the fundamental carbon fiber structure and material properties are established. The understanding of the conversion processes in the LT furnace, and the effects of spatial and temporal variations of the LT process parameters on the carbon fiber properties are necessary to identify possible process improvements and cost savings. The objective of this research was to develop computational models for gas flow and energy transport in the gas and fiber phases of the LT furnace, and to couple them with the fiber conversion process models. The model is implemented in the three-dimensional framework that enables analysis of process condition variations in all directions. The formulation is based on modified transport equation to simulate steady state conditions and thus significantly reduce computational effort associated with transient methods. The model is implemented in open source computational fluid dynamics (CFD) code OpenFOAM. The model has been demonstrated on a prototype carbon fiber LT furnace and can be extended to other geometries and process conditions. Extensions to other physical effects, such as accounting evolution of multiple gas species, and fiber tensioning are straightforward. The model uses High Performance Computing (HPC) capabilities of OpenFOAM and can be implemented on multi-processor workstations or mid-size computer clusters common in the industrial setting.

1. INTRODUCTION

Widespread use of carbon fiber in the automotive industry would need an annual production capacity of about a million tons of carbon fiber per year [up from the current maximum capacity of 100,000 tons/yr (TPY)]. It would also require the carbon fiber to be low cost, have reliable quality, large volume and higher speed production. In order to meet the efficiency, quality and volume targets, it is necessary to scale up carbon fiber lines by having larger furnaces, faster line speeds, and higher tow count. Processing calculations show that the current 'state of the art' 1500TPY carbon fiber line uses 30kW of energy to produce 1 kg of fiber. A scaled-up line capable of making 10,000TPY will need only about 12.5kW/kg, with more than 50% of energy savings with a commensurate savings in cost.

Building a carbon fiber production line is a capital-intensive undertaking that takes a lot of planning and a long implementation time [1]. Production lines are technologically complex and expensive to run due to enormous thermal energy requirements. The bulk of the energy is spent in eliminating non-carbon atoms from PAN fibers by oxidation (stabilization) and carbonization processes [2, 3]. Carbonization converts the stabilized oxidized PAN structure into carbon fiber structure with highly enhanced mechanical properties. The carbonization is usually conducted in two steps, in low temperature (LT) and high temperature (HT) furnaces.

In the industrial setting, the carbonization furnaces are horizontally oriented, continuous processing devices [4]. The PAN fibers are fed into the furnace at a constant speed, heated, and removed on the furnace exit. The fibers form a substrate that is heated by radiation from the furnace walls. The walls of the furnace form an enclosed space, referred to as a muffle, which separates heating elements from the furnace load, i.e. PAN fibers. The enclosure enables control of the processing atmosphere and separates the heating elements from the volatile tarry gases. Dwell time of fibers in the carbonization furnaces is determined by the kinetics of conversion and the heating rates. The carbonization furnace lengths vary, they are measured in meters and the dwell time is measured in minutes, compared to hours for the oxidation stage dwell times [1]. Multiple fibers are processed at the same time. The parallel fibers form a horizontal mat across the width of the furnace. Increasing the furnace width is considered as one of the most practical avenues for scaling up the carbon fiber production.

Inside the LT furnace, the main carbon fiber building blocks are constructed that establish foundation for the resulting mechanical properties [1, 5]. There, fibers lose about 50% of their weight which is the largest mass transfer in the carbon fiber production line. Fibers also shrink in diameter and contract about 10%. The heating rate has to be controlled to avoid damage to the fiber structure due to formation of gaseous decomposition species. The mechanical properties of the fibers are directly related to the perfection and uniformity of the turbostratic structure built during the LT carbonization [1]. LT furnaces have multiple heating zones, starting from the room temperature and increasing up to 800 C.

Compared to a wide body of research on the oxidative stabilization of PAN fibers [6-8], very little work has been done on the effect of process conditions in the LT carbonization stage on the fiber mechanical properties [1, 2, 5, 9]. The underlying thermochemical processes are still fairly obscure, and the role of LT processing parameters, such as thermal history and tension, on the extent of fiber conversion and its mechanical properties have not been systematically studied. The furnace temperature profile and the flow of gases are essential to achieving uniform fiber properties, which is the primary interest to the LT furnace manufacturers. Achieving consistent process conditions and the corresponding consistency in the carbon fiber quality across the width of the furnace is the major challenge in scaling-up production and reducing the manufacturing cost.

There are only few publications on device scale modeling the LT carbon fiber furnaces. The models developed by Harper Int. researchers [10-12] have been focused on the fiber conversion. The models are based on one-dimensional representation of a representative carbon filament under the steady state conditions in a multi-zone LT furnace. Energy balance on the fiber include energy transport by radiation, conduction and convection between the fiber and the furnace, and the energy of chemical reactions during the conversion process. The off-gas release during the conversion as a function of the temperature is

related to the fiber mass and cross-section reduction. The model shows limited sensitivity to the localized variations in the temperature history that may be expected from vents or other local perturbations in the flow field [12]. This may indicate a larger role of fiber tensioning that may be more sensitive to localized temperature variations because it is distributed along the entire fiber span in the furnace. Recent experimental study [13], investigated the role of tension and temperature on the resulting mechanical properties of the carbon fibers. They found that the two process parameters can be utilized to produce automotive grade fibers after the LT carbonization stage thereby eliminating the HT stage and reducing the overall energy costs. Reference [14], describes the only full three-dimensional model of the LT furnace developed so far. It employs a single phase, gas domain formulation. The fiber effects on the flow of gasses in the model are accounted for by a porous flow regime in the horizontal layers where fibers are supposed to be located. The radiative heating is based on the concentration of the grey gasses in the cells. Because the fiber phase is not directly modeled, temperatures of the gas in the porous zone were used to approximate the fiber temperatures, based on an assumption of thermal equilibrium between the gas and the fiber. However, as the grey gasses are the only absorber of the radiative heat in the model (which drives the temperatures in the fiber zones), the release of the off-gases from the fibers (or in this case fiber cells), is a consequence of the same off-gases released from the fibers. In addition, surface convective heat transfer between the fiber mat and gasses is not accounted for. To illustrate the causality, given that the purge nitrogen gas pumped into the furnace is not a big absorber of the infrared radiation, and assuming that the off-gas release from the fibers is artificially suppressed, the porous zone in the model that represents the fiber mat should not experience significant rise in temperature. The rationale for the equilibrium approximation and gas-based heating becomes less straightforward as the fraction of inert gases increases, and the thermal irradiation from the walls of the furnace directly into fibers dominate. An alternative modeling approach is to use combined gaseous and solid domains that directly account for the heating of the fiber phase by radiation from the furnace walls. As the concentration of fiber off-gases increase along the length of the furnace, they would increasingly occlude the furnace wall radiation into the fibers, and radiate and convect the furnace wall heat, hindering the primary fiber heating mechanism. Assuming that such effect is detrimental to the energy efficiency of the furnace, positioning of the furnace vents could be used to reduce it.

Specializations and implementation of computational models to processes that have not been in the mainstream of interest of the computational modeling community are not always straightforward. In this project we ended up pursuing three options and modeling frameworks. The first approach, as outlined in the original project plan, was based on a commercial CFD modeling software CONVERGE [15]. Due to the software vendor prioritization of development resources, the sub models necessary for simulating the LT furnace in CONVERGE were not implemented and we had to adjust the plans several months into the project. We then investigated the capabilities and feasibility of open source software MFiX (Multiphase Flow with Interphase eXchanges) [16] for modeling LT furnace. MFiX is a general-purpose hydrodynamic software developed by The National Energy Technology Laboratory (NETL) that describes chemical reactions and heat transfer in dense or dilute fluid-solids flows, flows typically occurring in energy conversion and chemical processing reactors. Although the initial results were encouraging, we found that for the given duration of the project it was not practical to implement the capabilities we wanted, which included the physics and the High Performance Computing (HPC) capabilities. With all the existing constraints, we finally settled on the third approach, OpenFOAM (Open Source Field Operation and Manipulation) [17], an open source software with a large user community, existing scalable fluid flow solver coupled with thermochemical transport, and overall strong HPC capabilities. In this report, we describe the development of the LT furnace model using the OpenFOAM framework. The work related to the first two approaches will not be documented, although it consumed a significant portion of the project resources. The lessons learned during those stages of the project helped us to accurately define the problem, and to test various approaches and assumptions.

One of the biggest challenges in this project was to select adequate models for governing physical phenomena and to create a simulation framework that would allow for incorporation of additional models with minor revisions to the overall approach. We have focused on implementing radiation and convection heating model in the fiber mat, and the mat interaction with the gaseous phase. The off-gas release from

the fiber during conversion along the length of the furnace is modeled by the one-dimensional formulation [12]. The off-gas is represented by a single gas compound, but the model can be easily extended with multi-component species transport model with chemical kinetics source terms. The off-gas is mixed with the purge gas and heated by convection against the fiber mat and furnace walls, and radiation. More complex models of radiation heating of grey gasses [18, 19] can be added, as the more complex off-gas release models are developed. In the following sections we first describe the essential characteristic of the problem, followed by the formulation of the model. The results of various model implementations illustrate the capabilities of the developed framework to model different aspects of carbon fiber carbonization furnaces.

2. PROBLEM DESCRIPTION

The LT furnace is the first step in the conversion of the stabilized/oxidized PAN fibers into the carbon fibers. The conversion is a pyrolysis process that requires an inert, oxygen-free atmosphere. To avoid Oxygen stripping of carbon from the fiber, purge chambers with pumped nitrogen gas [20] are placed at both entrances prevent ingress of outside air as shown in the Figure 1. The pyrolysis removes non-carbon compounds and create crystalline carbon structures that give the fiber its high mechanical stiffness and strength [1, 21]. The LT furnace usually have several heating zones with temperatures increasing away from the PAN fiber entrance. The heating rate has to be controlled to avoid formation of fiber defects by rapid formation of gaseous decomposition compounds [2]. The enclosing metal muffle of the LT furnace radiates heat into the fiber substrate and the furnace atmosphere. The heaters are placed above and below the muffle in order to create uniform temperatures in the muffle walls along the circumference. Side walls also act as radiation reflectors and reduce the non-uniformity of the heating at the edges of the fiber mat. Nitrogen purge gas is not an efficient absorber of the infrared radiation and the majority of the radiated heat may be apportioned to the fiber substrate. The deposited radiative heating energy increases the temperature of the stabilized PAN fiber and drives thermal conversion from stabilized PAN into carbon fiber. Matching the spectral output of the radiant source (muffle walls) with the spectral radiant absorptivity of the fiber as it moves through the furnace may be used to maximize energy efficiency of the furnace. The radiation heating depends on the geometry of the furnace. It the case of rectangular muffle cross-section, simple approximations can be used to relate intensity of the surface heating from the thermally radiating walls into the fiber mat [22]. LT furnace is a continuous processor with fixed muffle wall temperatures, and stabilized PAN fiber is fed into and out of the furnace at a constant rate. The process is therefore very close to a steady state which simplifies the analysis and measurements.

We have used the geometry and the operating conditions of the LT furnace from the Oak Ridge National Laboratory (ORNL) Carbon Fiber Technology Facility (CFTF) [23]. CFTF is 390-ft. long processing line, capable of custom unit operation configuration and has a capacity of up to 25 tons per year, allowing industry to validate conversion of their carbon fiber precursors at semi-production scale. The objective of the research project was to develop a three-dimensional, multi-physics computational model of the processing in the LT carbonization furnace that accounts for main processing effects outlined above. The model can be used for analysis of modification of processing conditions and furnace design to optimize processing conditions and energy efficiency of the process.

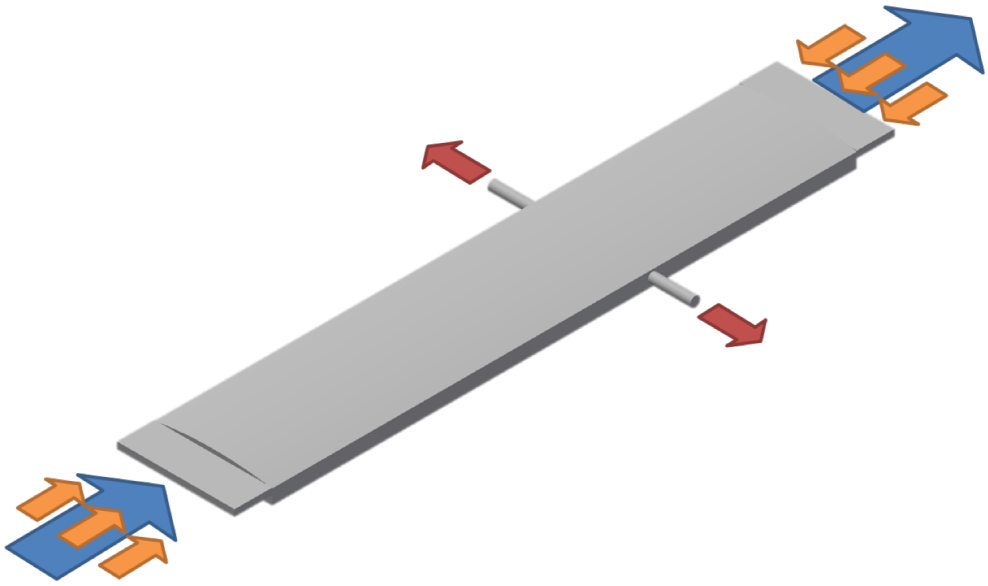

Figure 1 Schematic of LT furnace

3. IMPACT

The direct consequences of this work is the ability to use computational models as enabling tools for designing, building, commissioning and operating advanced Carbon Fiber production lines with a very high degree of confidence. Modifying furnaces after they are built is extremely expensive and sometimes not even possible. The comprehensive mathematical model, after it is validated, will help develop a blueprint for new, faster, more energy efficient processes which can enable the rapid introduction of carbon fiber reinforced polymer composites in the automotive world and then into other land-based transport systems.

Indirect or secondary impact of the developed computational modeling capability is relevant to many industrial fields. The low-cost carbon fiber manufacturing is not limited to carbon fiber manufacturing industry. New industries adapting carbon fiber product would be affected. In automotive industry, vehicles with Carbon Fiber Reinforced Polymer (CFRP) structural body and chassis replacing current steel material would consume less fuel with uncompromised safety features due to light weight. To achieve global energy savings light weighting by low cost carbon fiber becomes more attractive as the cost for carbon fiber is decreased. Wind energy farm would harvest more energy thanks to the longer blade design using low cost CFRP. Alternative fuel – CNG or hydrogen – passenger vehicle or public transportation might get its travel distance extended due to high strength pressure vessels that can store high pressure gaseous fuel. CFRP storage tank may provide enough gaseous fuel to next generation car such as fuel-cell powered vehicle. Impact of low cost carbon fiber is not limited to energy savings. It would enhance our daily life providing higher performance sporting goods and recreational equipment.

4. MODELLING APPROACH

The PAN based precursor fiber is subjected to many thermo-chemical processing steps that are driven by temperature control, such as stabilization, low temperature (LT) carbonization, and high temperature (HT) carbonization. An LT carbonization furnace is a continuous, radiative heating furnace with

controlled atmosphere that converts stabilized PAN into carbon fiber. The electric heaters heat the furnace muffle from the outside, which in turn radiates the heat into the moving fiber mat. A typical fiber residence time in LT furnace is 80 seconds during which they lose almost 50% of mass by off-gas release. To avoid charring during thermal decomposition, an inert atmosphere is maintained by pumping nitrogen gas through the muffle. The furnace process conditions during the LT carbonization step have important influence on the quality and uniformity of the resulting mechanical properties of the fiber.

The primary challenge in building wider, more energy efficient LT furnaces with increased capacity is ensuring uniform fiber properties across the width of the furnace. By increasing the furnace size, the spatial variations in the gas flow patterns and muffle wall temperatures may also increase, and thereby increase variation of the product properties. The number and locations of the exhaust vents, as well as heating control may be used to improve the consistency of the production process.

Previous studies have been focused on improving the tensile and yield strength of carbon fibers by optimizing the process parameters. The LT furnace operation involves a complex interplay of various phenomena such as compressible flow, radiation heating to fibers/off-gases, and chemical decomposition and mass loss of fibers. Though a three-dimensional fluid dynamics model of pyrolysis in LT furnace was developed earlier, it did not consider the off-gas release rates as a function of temperature history and amount of volatiles present during the carbonization of PAN fibers. A full-scale fluid dynamics model of the LT furnace with a realistic energy transfer, emission rates and mass loss at the fibers, we need to utilize HPC resources. To this goal, we present a development of the 3D model with off-gas emission rates as function of temperature considering the transient effects of moving fiber-tows. The off-gas release into the fluid domain is solved as species/scalar transport coupled with compressible flow.

Our LT furnace computational model has multiple, non-overlapping domains. The fiber tow domain is considered as moving media which undergoes radiative heating as well as thermo-chemical conversion. The model for gas domain uses compressible gas formulation with composition varying between pure gas to a mixture of chemically reacting off-gases species that absorbs heat due to infrared radiation and convection from fiber tows. An important part of the model development was to numerically validate the performance of the models used for the selected physical processes, and to evaluate their influence on the system-scale performance criteria. In this aspect, the OpenFOAM provided an excellent testbed to evaluate the various combinations of fidelity required in each physical process within the furnace scale model.

Our first step in the model development was to investigate approximation of the fiber mat as a porous membrane and its influence on the large scale flow features in the furnace. This was a critical step to move forward as we needed to determine the extent of computational mesh resolution and refinement. The tow bands thickness and porosity are determined by submicron scales, but their effects have to be homogenized in meters long furnace. Based on this study, we were able to determine the size of the production scale computational model meshes. The number of cells used in the models were of the order of millions, depending on the phenomena included in the models. Typical operation of LT furnaces has a ramped profile of the muffle temperatures, starting at 300° and ending in the 700 °C at the end of furnace. The muffle heats the moving fiber tows by radiation, and the colder purge gases take the heat away by convection. To model this interaction and to maintain the steady-state thermodynamic equilibrium we need to explicitly model the multiple tow-band regions in the furnace. By decomposing the domain into multiple phase regions, we introduced the shared boundaries that allow us to impose combined radiative and convective flux boundary conditions that couple the regions.

In the gas domain, the purge gas (nitrogen) is blown into the furnace through front and back inlets. In practice these flows rates may be different, but for this analysis they are assigned identical flow rates. Baseline nitrogen flow rate is assigned as a boundary condition of 0.5093 g/sec per inlet. The inlet temperature of the process nitrogen purge gas is set 300°C for both the front and back end of the system [10]. These gases mix with the off-gases released from the tow-bands giving rise to various gas phase compositions along the length of the furnace. We introduce a new gas phase model for representing these mixtures of two flows (nitrogen and pseudo-pure off-gas). The scalar variable (representing mass fraction

of off-gas) is set as zero for purge gas inlets. Scalar value of 0 is pure nitrogen, and scalar value of 1 is pure off-gas. Off-gas release rate is the flux boundary condition on the surface of the fibers. Since the mean molecular weights are similar for nitrogen and off-gas, the variable density is set as a function of temperature rather than mixing. As noted above, the release rate is a function of many physical quantities and related with chemical kinetics [14] of carbonization reaction. For this study we considered off-gas concentrations as a function of mass of volatiles and temperature based on work published by Fiedler et al. [24]. It was assumed that all four sides of rectangular tow-bands release off-gas at same rate.

Full-scale transient simulation of the LT furnace at the desired spatial resolution is not computationally feasible except on the large supercomputers. We have developed a model approximation to account for the thermal transients introduced by the fiber motion, and cast the problem using a steady-state formulation. Steady-state model of the LT furnace is computationally manageable on the computer cluster and multiprocessor workstations available in typical industrial settings. Earlier study [14] has modeled the fiber tow-domain as a gaseous phase with gas flow resistance due to fiber mat porosity. The model used a moving reference frame with linear velocity to model the effect of the fiber tow movement on the gas flow. The limitations of such approach, is that the radiative heating for the solid phase of fiber cannot be accounted for because the thermal mass of the tow-bands is not modelled. In the current study, we explicitly model the solid fiber domains and the corresponding thermal masses, which gives us ability to account for the energy transport and interactions in the system.

During normal operations, the continuous LT furnace attains a steady-state condition and has negligible temporal variations in the process conditions at any location in the furnace. Assuming absence of periodic eddies in the gas flow, temperature distribution of the muffle walls independent of time, and known fiber mat speed through the furnace, the state of the fiber segment in the furnace becomes a function of its location. In the steady state, the fiber properties at any location in the furnace are result of accumulation of all the incremental changes that fiber underwent from the time it entered into the furnace to its current location. For a known fiber mat speed, the current residence time of an infinitesimal fiber segment volume can be expressed by its current location. Figure 2 depicts the relation between the time, location and process history of the fiber segment dx moving from entrance at $x = 0$ up to its current location $x = x_i$.

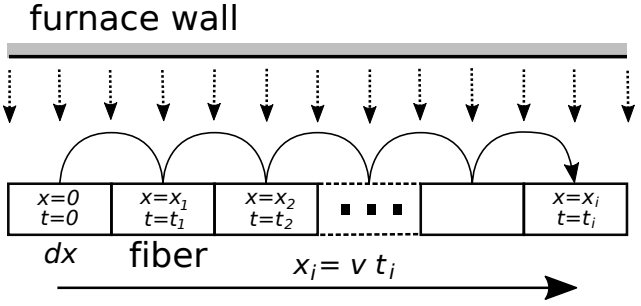

Figure 2 Relation of fiber state to its location in the furnace for a steady state model.

In a steady state model, the fiber properties at the entrance, $x = 0, t = 0$, are equal to the properties of the stabilized PAN fiber. As the fiber segment moves to location, $x = x_i$, at constant speed v, it goes through locations $x_i, x_i, \ldots$, during time interval $[0, t_i]$. The changes that the fiber segment experiences are accumulated into its current state at location x_i. The resulting property S at location x_i is an integral of the segment's rate changes as:

$$S(x_i) = \int_0^{t_i} S'(t)dt = \frac{1}{v}\int_0^{x_i} S'\left(\frac{x}{v}\right)dx$$

where S' denotes rate of change (kinetics) of property S. In the steady state model, the distribution of the fiber properties in the furnace can be calculated from the one-dimensional fiber conversion model [11] with assumed boundary conditions from the furnace model. A Picard iterative solver then alternates between the three-dimensional furnace model and the conversion model until the consistency between the two is achieved.

5. MODEL DEVELOPMENT AND SIMULATIONS

The computational domains that were generated during the course of the project were based on 1) prototype furnace from Harper International which has dimensions of 14 in length and 3 meters in width, and 2) LT furnace at CFTF facility located at the Oak Ridge National Laboratory which has dimensions of 4 meters in length and 40 cm in width. In the first problem geometry a cold flow simulation with porous regions representing the fiber tow are utilized. The second problem geometry consists multiple oxidized membranes of 30 mm width and are heated by radiation from gradual muffle wall temperatures of 375 C, 410 C, 475 C, 535 C, 600 C in separating flow chambers. The exhaust is located along the furnace length near the 3rd zone. One of the objectives of this project was to study the effect of the position of exhaust vent or vents in the furnace. For the initial study, using these OpenFOAM utilities, we generated three computational models with varying locations of the exhaust in the furnace. We used this feature to investigate sensitivity of the exhaust vent location and to demonstrate the parametric meshing capability. The first two cases correspond to single vent and to double vent on opposite ends along the length of the furnace. The final case was for a single vent on the top of the furnace. To enable parametric definition of the vent positions, a script was created that generates the inputs for the OpenFOAM utility blockMesh. The blockMesh utility creates parametric meshes based on the information provided from a dictionary file named blockMeshDict. The blockMesh utility decomposes the domain geometry into three-dimensional hexahedral cells. Following the blockMesh, we run a series of OpenFOAM utilities such as topoSet, createPatch and splitMesh to generate a multi-domain hexahedral computational mesh comprising of the flow domain and the fiber domain. A complete set of OpenFOAM utilities and workflow associated with this application is provided in the Appendix section.

5.1 3D COMPRESSIBLE FLOW MODEL

The initial study was conducted using the turbulent compressible flow formulation and modeling the fiber tows as porous membranes. The primary influence on the gas flow in the furnace is by the multiple equidistant fiber tow-bands where each band is a collection of fiber filaments, with dimensions around 4 cm wide and 10 microns in thickness. Resolving each and every fiber tow in a full-scale furnace model is computationally expensive. On the other hand, neglecting permeability of the tow bands could result in under-resolved interactions with the flow field. To understand the influence of anisotropic permeability of the tow-bands on the off-gas flow distribution we conducted a cold flow simulation study using the compressible turbulent flow in the gas domain and with PAN fibers modeled as porous media using a Darcy-Forchheimer relation. The porous media equations can capture the viscous losses and pressure drop across the permeable fiber mat. The existing steady-state solver within OpenFOAM (rhoPorousSimpleFoam) for turbulent compressible flows with implicit or explicit porosity treatment was used. The Reynolds Averaged Navier-Stokes (RANS) [25] solver is a standard industrial CFD technique used for analysis of turbulent flows. The time averaged momentum equation is given by equation (1) where the 'ρ' is the density, 'u' is the flow velocity, 'p' is the pressure, 'μ' is the viscosity and $\bar{\tau}_{ij}$' is the mean rate of stress tensor defined by equation (2). In this solver, porous membrane is modeled by adding a sink term to the Navier-Stokes equations. The source term 'S_i' given in the equation (3) is composed of two parts, a viscous loss term and an inertial loss term, creating a pressure drop that is proportional to the velocity and velocity squared, respectively.

$$\rho\bar{u}_J \frac{\partial(\bar{u}_\iota)}{\partial x_j} = \rho\bar{f}_i + \frac{\partial}{\partial x_j}\left[-\bar{p}\delta_{ij} + 2\mu\bar{\tau}_{ij} - \rho\overline{u_i' u_j'}\right] + S_i \quad (1)$$

$$\bar{\tau}_{ij} = \frac{1}{2}\left(\frac{\partial\bar{u}_\iota}{\partial x_j} + \frac{\partial\bar{u}_j}{\partial x_i}\right) \quad (2)$$

$$S_i = -\left(\mu D_{ij} + \frac{1}{2}\rho|u_{kk}|F_{ij}\right)u_i \quad (3)$$

The implicit porosity solver is computationally more robust and is needed if the flow resistances are large, heavily anisotropic or not aligned with the global coordinates. The fiber tow domain does not differentiate individual fibers but treats them as an equivalent media with anisotropic permeability along the fiber lengths included into the LT furnace. Anisotropy in permeability of the tow bands has been introduced. The muffle walls are held at constant temperature. The flow conditions and N_2 injection rate were chosen to correspond with the steady state conditions of the LT furnace. A reference pressure boundary condition is imposed on the outlet of the domain. The flow properties and thermochemical properties of off-gas were provided by Harper International [10]. The Figure 3 shows the streamlines color coded with velocity contours for different vent locations. A simple verification of the flow rates at the inlet and exhaust is used to verify the conservation of mass. The model with parametric location of vents provides a great capability to study the recirculation/dead zones and residence times of gas in the furnace.

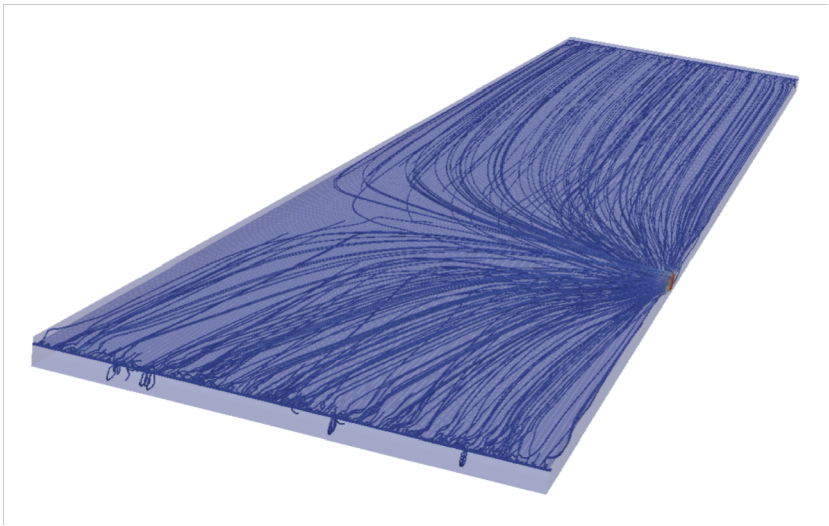

(a)

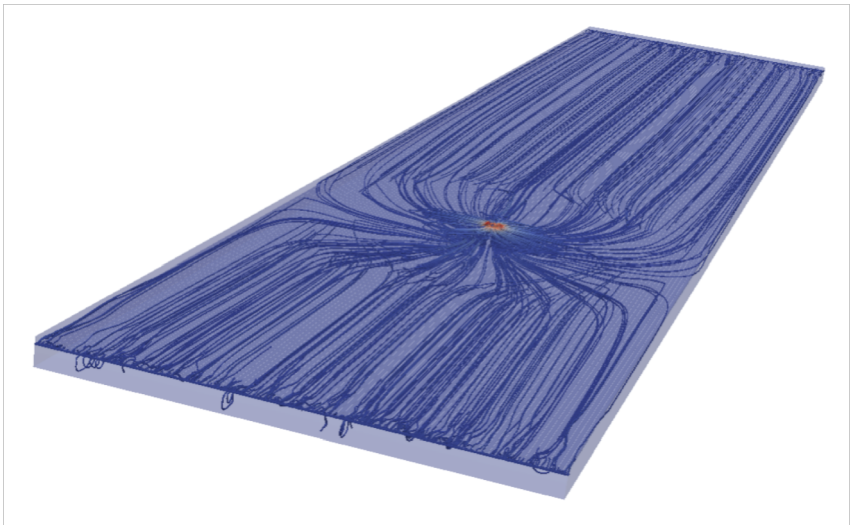

(b)

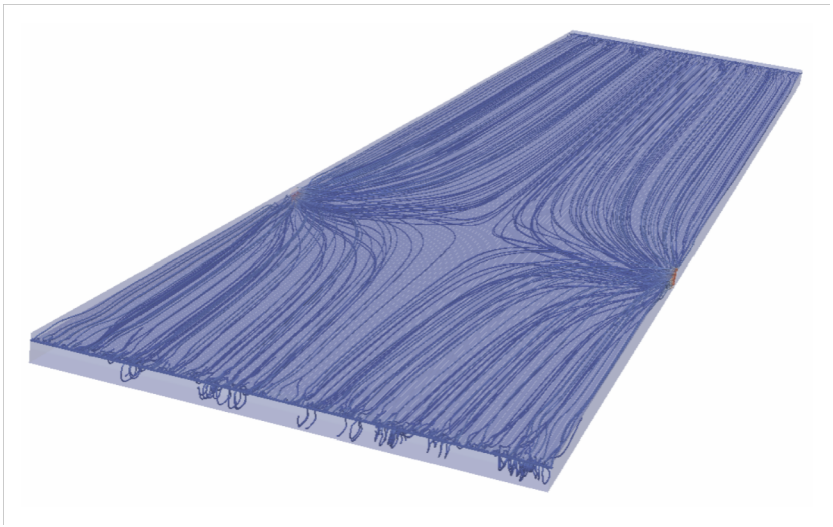

(c)

Figure 3 Streamlines of off-gas to study the sensitivity of vent location on residence time and dead zones, (a) side, (b) top, and (c) both sides

5.2 CHEMICAL COMPOSITION OF OFF-GAS AND 1D FIBER CONVERSION MODELING

In the previous section we have described development of a furnace cold flow model that regards the fiber tows as a permeable porous zone. In this section we describe the development of a new model that treats multiple fiber tows as separate solid regions with thermal mass and inserts the spacing between the tows as the gas phase. During the thermal decomposition process of oxidized PAN fibers heated by radiation, the new chemical gaseous species are generated (off-gas) and transported within the furnace [2]. The transport of the chemical species occurs by convection, which is impacted by the flow of purge gases; and diffusion, which depends on the chemical interaction between the gases. A scalar transport equation is coupled to the compressible flow to track the concentrations of the off-gas that is released

from the fibers due to pyrolysis. The current model assumes two species, N_2 and off-gas. In this simulation we model off-gas as a single species gas (methane, CH_4) and the account for mixing of the two gases (nitrogen and methane). The single species off-gas is a placeholder at this time since we do not have a multi-species reaction model for the fiber conversion in the LT furnace. In the scalar transport solver in OpenFOAM, the composition of a mixture is modeled by a fraction variable which defines the state of the off-gas mixture on a scale ranging from 0, corresponding to pure N_2, to 1 corresponding to pure off-gas.

In order to properly account for the heat transfer interactions between the fiber and the furnace environment that drive the pyrolysis, we explicitly modeled the fiber tow regions as solids, so that the fibers can be heated directly by radiation. The fibers are radiatively heated by the furnace walls and interacting with the gas phase primarily by convection cooling. We modeled the furnace muffle radiation as heat sources for the fiber and gas, and used conjugate heat transfer model to cool the fibers convection of N_2 gas. A complete set of conservation of energy equation and scalar transport of species are solved in all regions. The energy and scalar balance equations consists of accumulation over time, convection, diffusion, and source terms. The common forms of energy conservation equations are cast in terms internal energy '*e*' and enthalpy '*h*' that are based on constant volume and pressure conditions, respectively. For gas phase under constant pressure, a suitable measure for energy conservation is enthalpy. The Reynolds averaged conservation of energy for turbulent compressible flow in enthalpy form is given by equation (4). The thermal diffusivity is given by equation (5) where μ is the viscosity given by Sutherland's Law. The source of enthalpy equation can be contributed by radiation heating and represented is by $\dot{\omega}_{rad}$ term.

$$\frac{\partial(\rho\bar{h})}{\partial t} + \frac{\partial(\rho\bar{u}_j\bar{h})}{\partial x_j} = -\frac{\partial}{\partial x_j}\left(\rho\alpha\frac{\partial\bar{h}}{\partial x_j} - \rho\overline{u_j h}\right) - \frac{\partial\overline{q_r}}{\partial x_i} + \dot{\omega}_{rad} \tag{4}$$

$$\rho\alpha = \mu\frac{C_v}{C_p}\left(1.32 + 1.77\frac{R}{C_v}\right) \tag{5}$$

For a mixture of multiple species, a transport equation for the mean mass fraction of an individual species Y_s can be defined according to,

$$\frac{\partial(\rho\widetilde{Y}_s)}{\partial t} + \frac{\partial(\rho\widetilde{Y}_s\bar{u}_j)}{\partial x_j} = \frac{\partial}{\partial x_j}\left(\left(\rho D_{m,s} + \frac{\mu_t}{Sc_t}\right)\frac{\partial\widetilde{Y}_s}{\partial x_j}\right) + \dot{\omega}_s \tag{6}$$

Based on Fick's law, the diffusive flux of chemical species is proportional to the gradient of the mass of the species, where $D_{m,s}$ is the mass diffusivity of species '*s*' and $\dot{\omega}_s$ represent the chemical reaction source term, which can be either generation or consumption of the species. The chemical reaction source term is calculated by the reaction rate law which describes the mass change of a species over time. i.e., generation or consumption of chemical species $\widetilde{Y}_s$. This rate law is commonly expressed in Arrhenius form, an exponential relation that relates reaction rate to be proportional to the concentration of involved species and temperature with a power of specific order. The pyrolysis of the fiber regions due to radiation in inert gas environment involves multiple reactions in different temperature compartments of the LT furnace. However, since the conversion reactions are not well known, we model the process as a single step reaction with release of a representative off-gas into the furnace chamber. A detailed multi-step reaction mechanism can be easily added in the existing model, as needed. The increased number of modeled chemical reaction tends to disproportionally increase the computational effort, but the balancing between accurate modeling of chemical kinetics and numerical expediency is a commonplace in thermochemical analysis. From the fiber conversion model developed by the Harper Intl. [11], the off-gas

release rate is converted to mass flux source along the length of the fiber. This single species model for off-gas that will be added into the model, assuming without reactions with N_2 purge gas.

The fiber energy balance with sensible heat effect, enthalpy change for evolved gas, and heat transfer with its surroundings is given by

$$\frac{\partial(\rho_f \vec{u}_f \cdot \vec{A}_f \vec{h}_f)}{\partial z} = \frac{\partial}{\partial z}\left(\lambda_f A_f \frac{\partial T_f}{\partial z}\right) + \pi d_f\left(\alpha(T - T_f) - \dot{m}_s'' h_{s,v}\right) + \dot{q}_{r,abs} + q_{r,emission} \quad (7)$$

Where $\vec{h}_f$ is the fiber enthalpy, λ_f is the thermal conductivity, T_f is the fiber temperature, α is the heat transfer coefficient and $h_{s,v}$ is the enthalpy of the volatiles in fiber. Though carbonization might be continuous series of chemical reactions rather than clearly distinct single process, a 2-discretized-zone model has been developed for the sake of simplicity [11]. The fiber enthalpy is related to temperature as follows, where C_{pf} is the specific heat capacity of fiber and C_{po} is the specific heat capacity of volatiles in fiber.

$$\vec{h}_f = \int_{T_{ref}}^{T_f} \left((1 - Y_s)C_{pf} + Y_s C_{po}\right)\partial T \quad (8)$$

In the case of LT furnace that operates around 1000 K, the radiative heat transfer has higher contribution when compared to convective and conductive heat transfer. Heat transfer due to surface-surface radiation from the furnace muffle walls into the fibers, and convective heat transfer of the purge gas flow is modeled using mixed boundary condition formulation. A more complicated radiation models, such as view factor approach, can be employed as needed to include geometric factors when designing furnaces with varying cross section or with large temperature variations in the walls. At the steady state approximation, all the fluxes due to convection, conduction and radiation are assumed to be in equilibrium. We linearize the radiative flux contributions to the fiber and impose the total heat flux as a mixed boundary condition on the fiber surface. This nonlinear relation for the mixed boundary condition can be implemented using OpenFOAM utility swak4Foam that allows user defined function to be used in the definition of a boundary condition term. With this shared library, it is possible to define variables and functions on the boundary that are calculated at every internal iteration and use all available fields and additional helper functions such as magnitude or delta. The temperature at the cells center and face along the boundaries of fiber region are defined by T_c and T_f, temperatures of the flow domain and wall region are denoted by T_{flow} and T_∞ , ϵ is the emission coefficient and σ is the Stefan-Boltzmann constant.

$$q_{rad} = \epsilon\sigma\left(T_f^4 - T_\infty^4\right) = \epsilon\sigma\left(T_f^2 + T_\infty^2\right)\left(T_f^2 - T_\infty^2\right) \quad (9)$$

$$q_{rad} = h_{rad}\left(T_f - T_\infty\right) \quad (10)$$

$$h_{rad} = \epsilon\sigma\left(T_f^2 + T_\infty^2\right)\left(T_f + T_\infty\right) \quad (11)$$

$$q_{conv} = h_{conv}\left(T_f - T_{flow}\right) \quad (12)$$

The final form of the mixed boundary conditions at the fiber surfaces is given by the following equation, where the fractionExpression defined by user as (14) and δ is the distance between the cell center and cell face.

$$T_f = fT_\infty + (1-f)\left[T_c + \left(\frac{h_{conv}\delta}{k}\right)T_{flow}\right] \tag{13}$$

$$f = \frac{h_{rad}\delta}{k + \delta(h_{conv} + h_{rad})} \tag{14}$$

Another significant absorber of the muffle radiation heat are the off-gases as they contain mixture of grey gases, HCN, CO and CO_2 that can absorb radiant heat. The heating of the off-gases released due to radiation, $\dot{\omega}_{rad}$ in equation (4), can be modeled in OpenFOAM as volumetric heat source. The radiative source term in energy balance equation is the sum of the extent of gained and lost heat due to absorption and emission. The scattering effect is not accounted since it only redistributes radiative energy among the directions, not change the extent of local energy. Due to its simplicity, low computational cost with reasonable accuracy, the P1 model is used in the present work. The P1 radiation model is the simplest case of the more general spherical harmonics P-N model [26, 27]. Its basic premise is that the heating intensity in a participating medium can be represented as a rapidly converging series of orthogonal spherical harmonics. In P1 approximation only zeroth and first order moments of the intensity are used. The accuracy of P1 model is high if the radiation intensity in the system is mostly isotropic. The radiative heat loss q_r is calculated as,

$$\nabla q_r = \alpha_c G - 4\epsilon\sigma T_f^4 \tag{14}$$

Where α_c is the absorption coefficient (m^{-1}), ϵ is the emission coefficient (m^{-1}) and σ is the Stefan-Boltzmann constant. The incident radiation G is modeled according to

$$-\nabla\left(\frac{1}{3\alpha_c}\nabla G\right) - \alpha_c G + 4e_c\sigma T_f^4 = 0 \tag{15}$$

Next, we briefly describe the fiber conversion model developed by Lee et.al [10-12] to complete our numerical model. Fiber mass loss in LT furnace is a critical step that needs to be incorporated in the model. Any change in properties along the transverse direction is caused by interaction with surroundings rather than internal-gradient. With this assumption, 1D fiber model coupled with surrounding 3D flow conditions might be necessary to study transversal uniformity of the fiber tows. The mass transfer from fiber to gaseous phase, also known as mass loss of the fiber is given by the conservation equation,

$$\frac{\partial(\rho_f \vec{u}_f \vec{A}_f Y_s)}{\partial z} = \pi d_f \dot{m}_s'' \tag{16}$$

Where z is fiver moving direction coordinate, $\dot{m}_s''$ is mass transfer flux from solid to gas. In this equation ρ_f is the fiber density, $\vec{u}_f$ is the fiber velocity vector, $\vec{A}_f$ is the surface area vector of the fiber surface parallel to the flow direction, Y_s is the mass fraction of the solvent *s* in the fiber and d_f is the fiber diameter. Though there are many kinetic expressions available for thermal degradation of polymer [11], it has been reported that the first order kinetic relation is in good agreement with experiments. The $\dot{m}_s''$ is mass loss rate per volume defined by,

$$\dot{m}_s'' = Ae^{\left(\frac{-E_A}{RT}\right)}\left(m - m_f\right) \tag{17}$$

Where A is pre-exponent factor, E_A is activation energy, R is gas constant and m is mass of fiber, subscript f denotes final state and subscript o denotes initial state. Finally, the catenary formation is based on tensile forces in the fiber that are applied near the inlets and result elongation of the fiber and changing the physical properties. A force balance for a differential fiber element gives the equation of change of momentum in the fiber.

$$\frac{\partial(\rho_f \vec{u}_f \vec{u}_f \vec{A}_f)}{\partial z} = \frac{\partial \vec{F}}{\partial z} + \vec{F}_{fric} + \vec{F}_{gravity} \tag{18}$$

Combining all these models over a large-scale domain requires HPC resources. The momentum balance or Navier-Stokes equation contains two fields, pressure and velocity, that have a highly nonlinear relationship and need to be resolved simultaneously. The treatment of pressure-velocity coupling has to be considered carefully to minimize numerical error. The method used in these simulations, Semi-Implicit Method for Pressure-Linked Equations (SIMPLE) [28] is based on de-coupling the pressure and velocity fields. This allows us to calculate them separately, then use one field to correct another field iteratively until convergence achieved. The convergence of the numerical solver when using a SIMPLE algorithm where the solver has to iterate between the fiber regions and flow domains is evaluated. We are required to compute with over 500 outer iterations for achieving a steady state solution in the flow domain with residuals less than 10^{-4} and maintain thermal equilibrium with the fiber domains.

To test the model, we have setup a model of a small furnace with four equally spaced fiber tow bands in full furnace length. For these test simulations, we get an estimate of the mesh resolution of 6 million cells that are required to resolve the flow near the walls and fiber regions of the furnace at full scale. The wall temperature of the furnace is increased gradually in five zones as shown in Figure 4a. The Figure 4b below shows the methane gas fraction distribution over the length of the furnace color coded with the temperature of the four tow bands. As the nitrogen gas is pumped at the constant mass flow rate through both inlets, methane is released based on the temperature history of 1D fiber conversion model along the length of the fibers [11]. In this Figure 4b we can see the 3D rendering of fiber tows being heated due to radiation gradually along the length of the furnace and consequently off gases released has higher concentration around the vicinity of the fiber tow-bands. Also, we could see the concentration rise near exhaust around the 3rd furnace zone. The Figure 5a-b shows the nitrogen and methane distribution along the length of the furnace computed using a steady state compressible RANS simulation. As the nitrogen enters at the furnace the fraction of N_2 near the inlets are maximum. Also, we could see the flow structures develop along the length of the furnace. Now the off-gases (CH_4) are released based on the release rate from the fiber model discussed earlier. As the heat starts to build in the fthe fiber domain from the heat radiation, the off-gases are released based on the temperature dependent release rates and flow towards the exhaust vent. Though the primary physical processes were successfully demonstrated on the initial test prototype where the width of the domain could hold four fiber tow bands, we do not expect to see full scale flow re-circulations, stagnation zones in the volume plots.

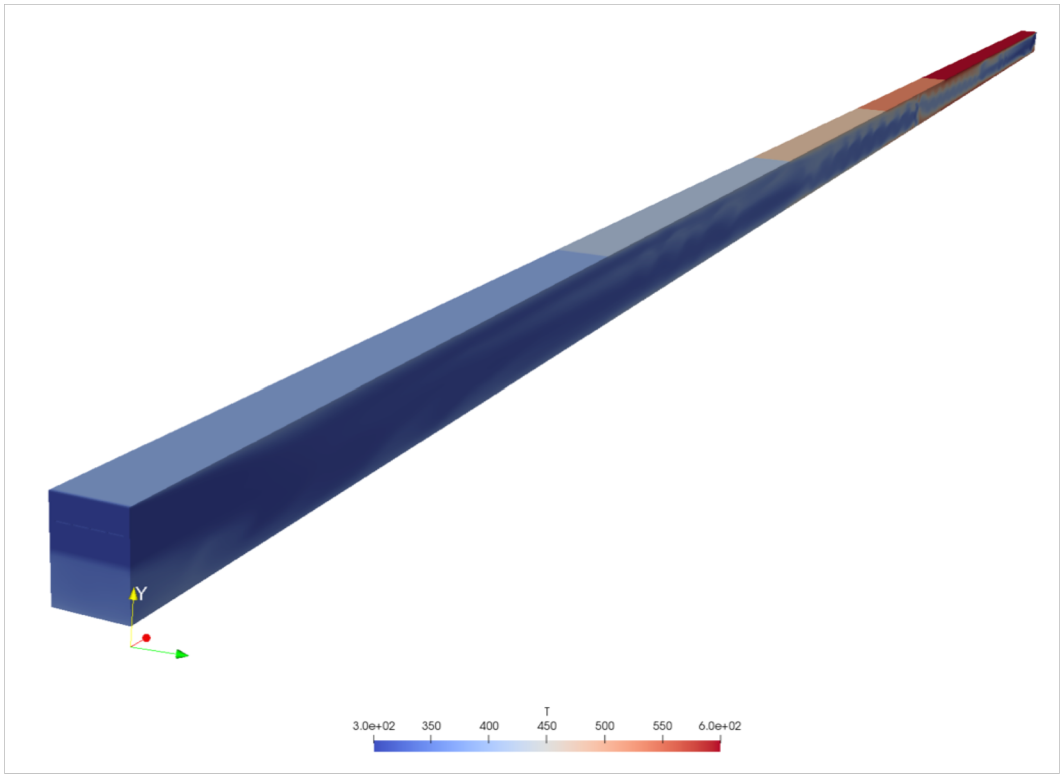

(a) Temperature plots

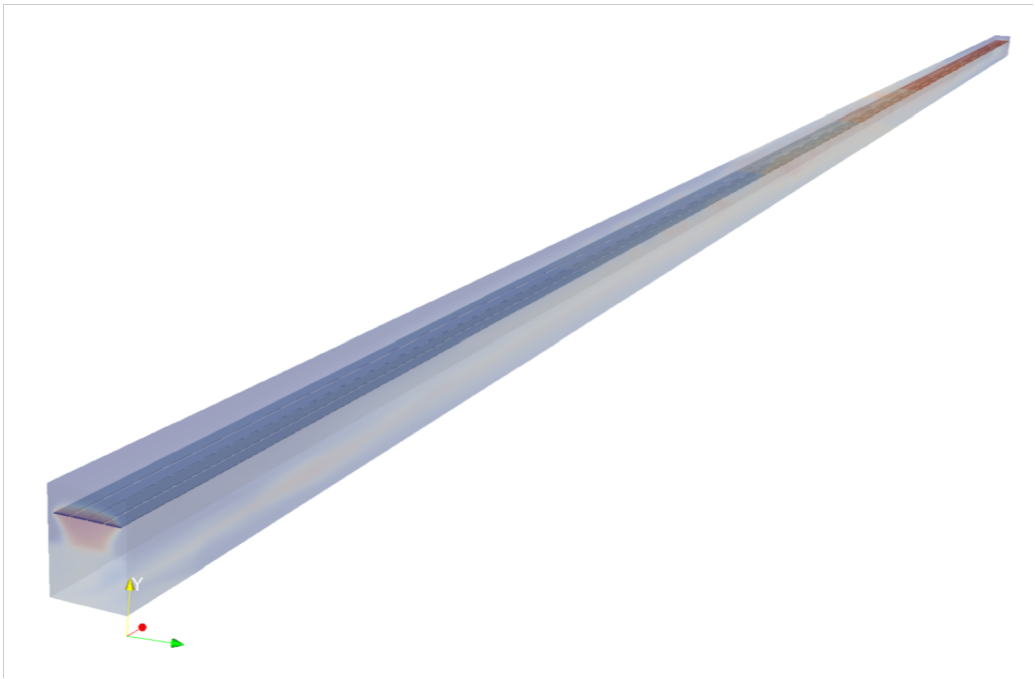

(b) CH_4 distribution

Figure 4 Volume rendering of the fields over the length of the furnace color coded with the temperature of the four tow bands

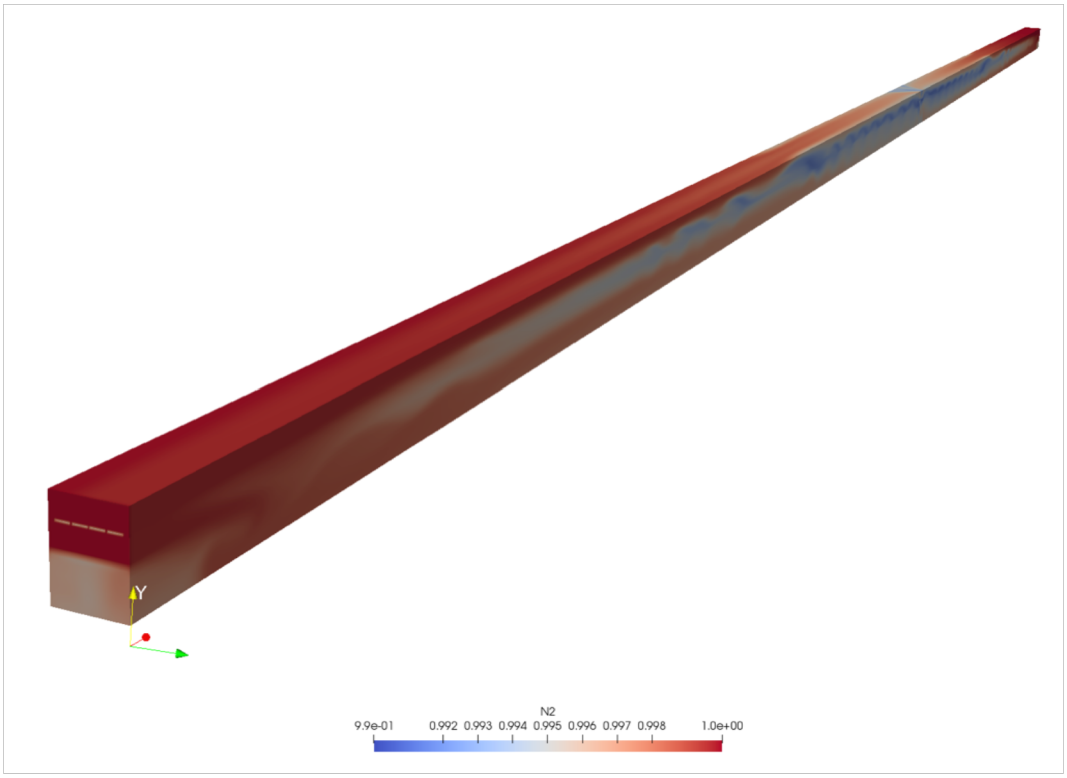

(a) N_2 distribution

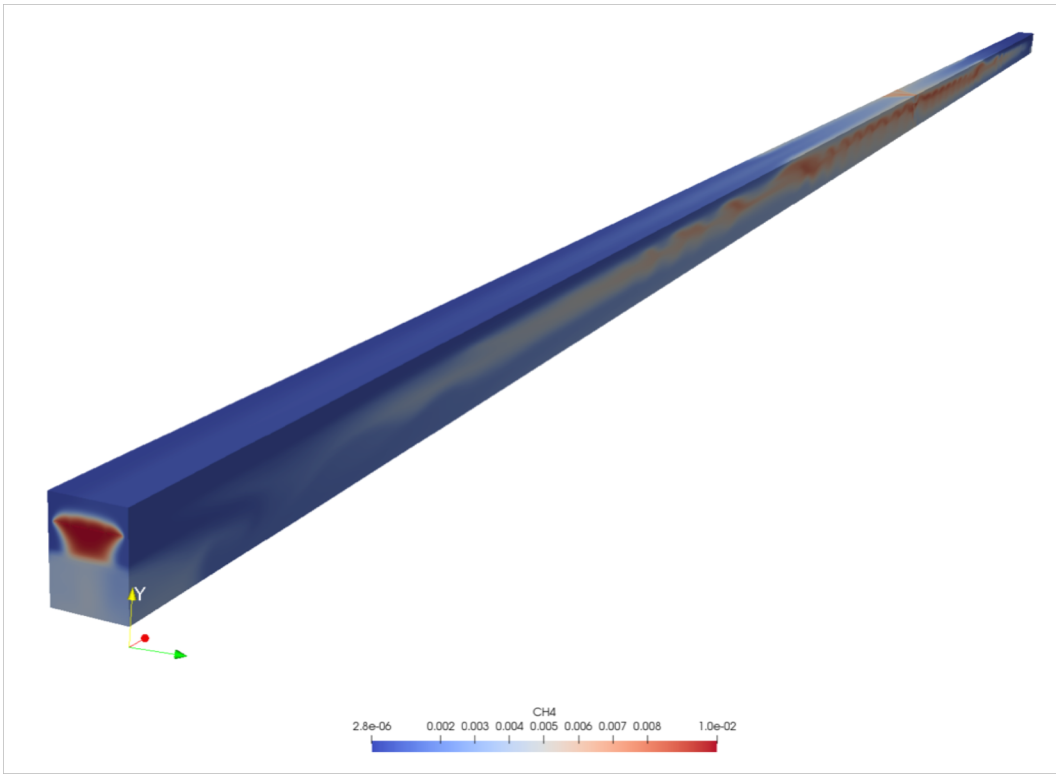

(b) CH4 distribution

Figure 5 Volume rendering of the fields over the length of the furnace color coded with the temperature of the four tow bands

5.3 CFTF LOW TEMPERATURE FURNACE MODEL

To demonstrate the capability of the current model formulation, we have conducted a study on the full-scale model of the LT furnace at CFTF facility with the fiber tow domains resolved. The geometric model is constructed based on the dimensions in the facility's technical drawings. The figure below shows the actual geometric model with 8 tow bands with 3 mm spacing in between them. The mesh resolution required to conduct a resolved RANS simulation for this geometry is around ~28 million cells.

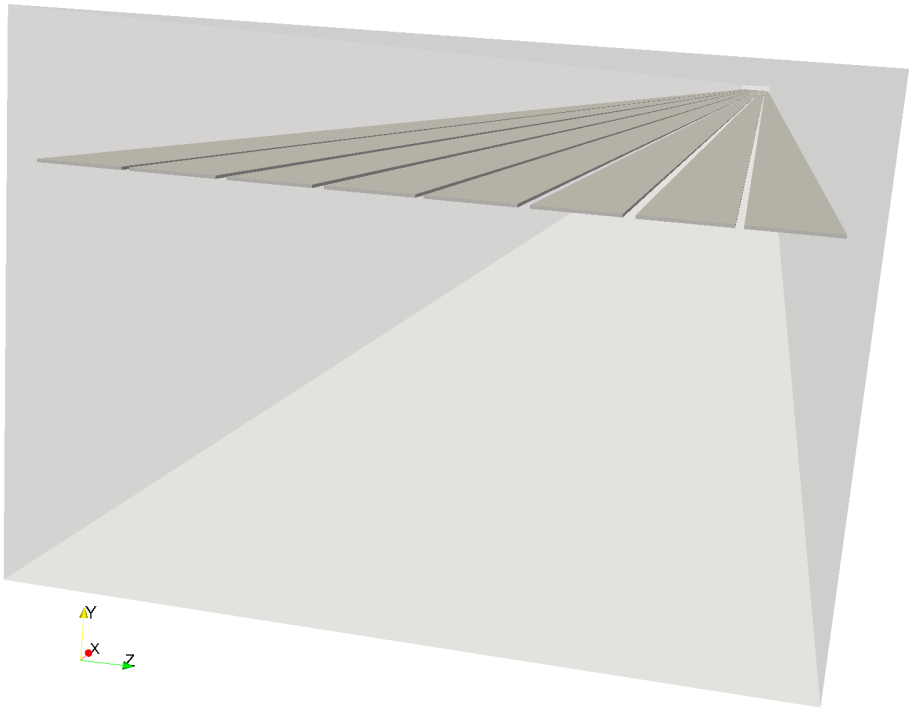

(a) 3D fiber resolved geometry

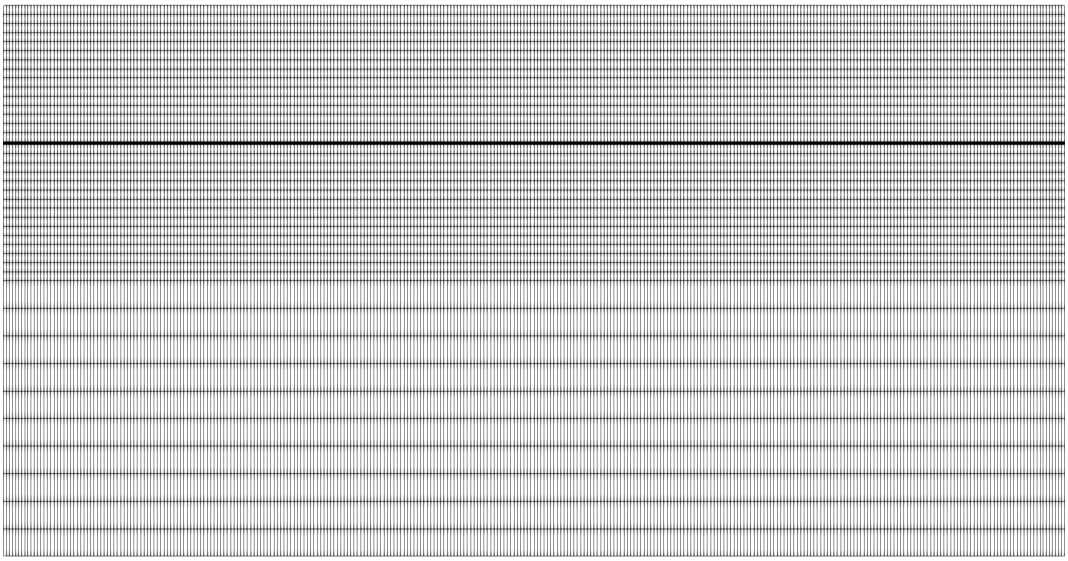

(b) Mesh resolution across the width

Figure 6 Computational domain and problem setup

In order to include the effect of fiber movement on the temperature distribution in the steady-state model, we implemented an algorithm modifying the equation of energy transport in the fiber region. The modification is based on the difference in the thermal energy contained in a fiber segment as it moves from one location to the next.

We model the energy transport generated by the movement of the fiber segment by using the transient transport term (or equivalently, thermal energy advective term [29]) to the right-hand side of equation (4) as a heat sink, as follows:

$$S_{adv} = -c_P\,\rho\frac{\partial T}{\partial t} = -c_P\,\rho\frac{\partial T}{\partial\left({}^{x}/_{v_f}\right)} = -v_f\;c_p(x)\;\rho(x)\frac{dT}{dx} \tag{19}$$

where $c_p(x)$ and $\rho(x)$ denote the effective fiber heat capacity and fiber density at location x, respectively. The sink expression in equation (19) requires knowledge of the gradient of temperature in the movement direction or, equivalently, the gradient of the fiber enthalpy. To avoid introducing and solving for another implicit relation in the model, and given that the radiative heating from the furnace muffle controls the fiber temperature, we use the gradient of the muffle wall temperature as an approximation, as shown in Figure 7.

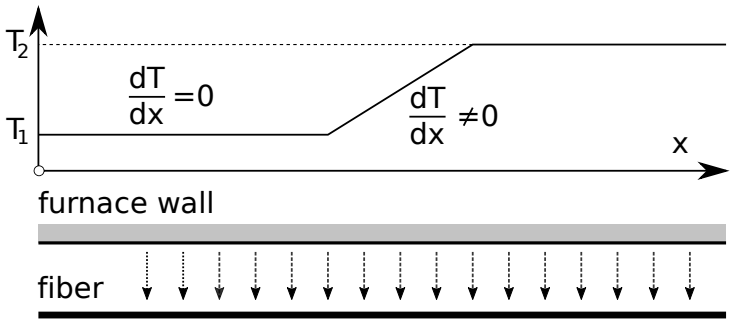

Figure 7 The effect of fiber movement on temperature.

Therefore, in the current formulation, the energy sink due to the fiber movement is active only in the regions between the different thermal zones in the furnace. A better approximation can be made by using a view factor radiation model.

The RANS simulations were conducted with $k-\Omega$ turbulence model to capture large scale flow structure and turbulent mixing of the off gases, and radiation heating until a steady state solution was reached. The figures show stream tracers and temperature planes across the width at three different locations along the length. In Figure 8a shows the gas flow stream tracers color coded with off-gas (CH_4) fraction distribution. We can see the stagnation region on the wall opposite to the exhaust where the off-gas fraction is maximum. Also, the regions in the lower half of the furnace chamber right next to the inlet muffler we see flow recirculation. This indicate the off-gases could be trapped in these regions during the carbonization process leading dead zones where the purge gas flows have lower influence. Also, the cut plane in the center show the temperature variation of the off-gas near exhaust. This the blue color in the lower region indicates the temperature values in the range of 400 K. This is probably not the case within the furnace as the radiation is dominant and at the exhaust the composition is primarily dominant by the off-gases which are hot. Figure 8b shows the heating in fiber tow bands due to radiations and non-uniform temperature distribution due to exhaust location. This could be caused due to higher flow rate near the exhaust leading to increase in velocity profiles and subsequently convecting more heat from the

fibers. The temperature non-uniformity could lead to carbonization delay of the fibers across the width as they proceed toward the exhaust and eventually leading to fibers with different physical properties.

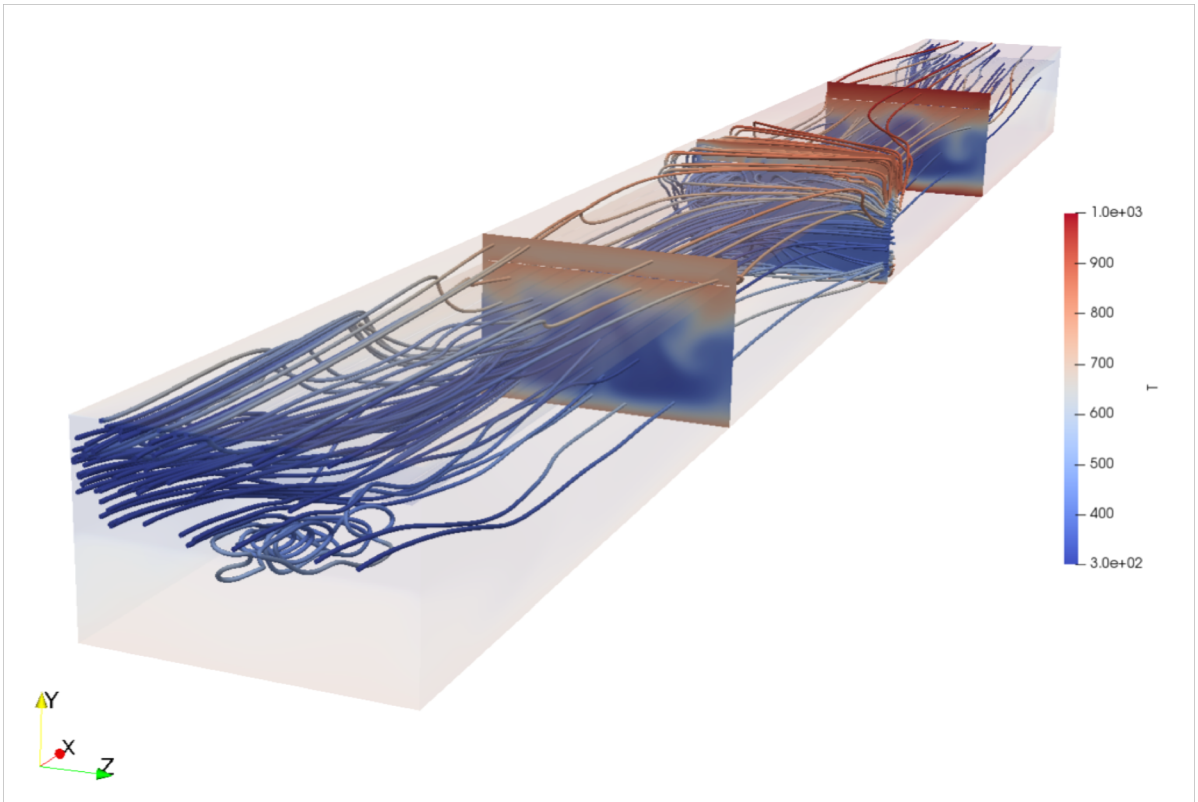

(a)

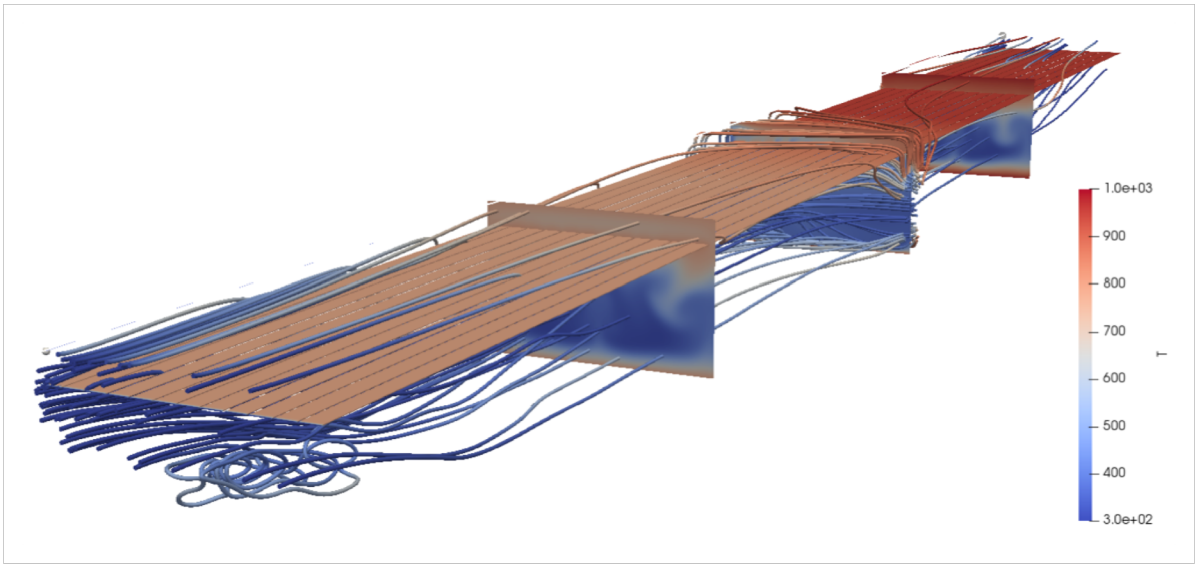

(b)

Figure 8 Streamlines color coded with off-gas concentration with cut-planes and fiber tows colored based on temperatures

The Figure 9a shows the temperature profiles along the length of each fiber. The inset shows the variation in temperature along the width of the furnace. This is primarily due to convection of heat as we have not considered geometric effects in radiation sources. Figure 9b shows the difference in temperature profile due to addition of fiber movement history into heat sink term. Due to addition of this term there is a delay on the temperature which could lead different chemical conversion mechanism. This feature allows for parametric study of the process line speed in trying to understand the dependence of line speed on the conversion of PAN fiber under carbonization. Figure 9c shows the gas phase temperature profile in the vicinity of the fiber regions. This shows the rise in flow temperature primarily due to convection from fiber which in turn is heated due to radiation. Also, we could see a dip in the temperature at the middle of the furnace indicating the location of exhaust where the mixing of upstream and downstream gases occurs.

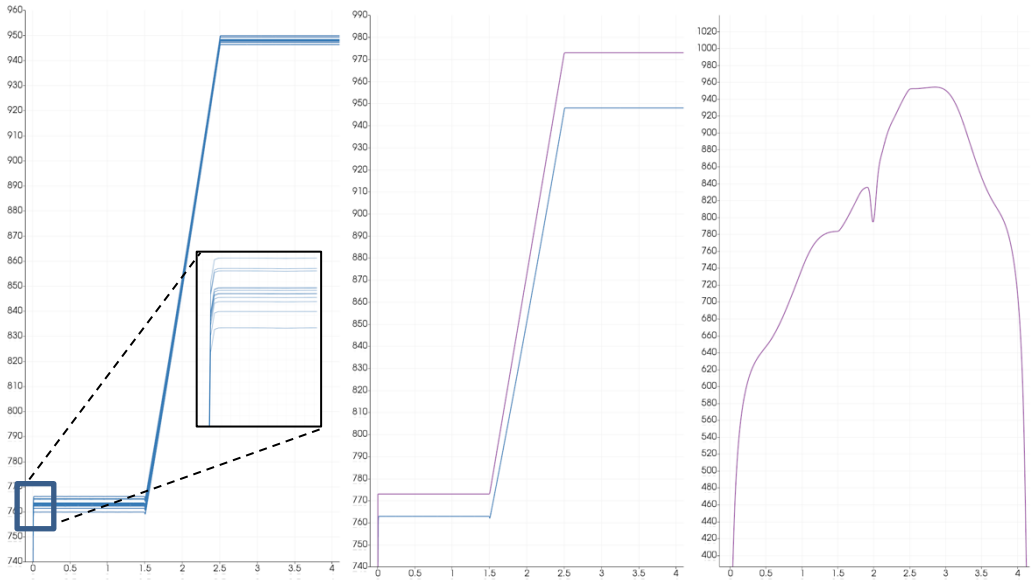

Figure 9 Temperature lineout along the length of the furnace on the multiple fiber tows

6. CONCLUSIONS AND FUTURE WORK

We have developed a computational model for the carbonization furnaces using open source software OpenFOAM. The model accounts main physical and chemical processes in the furnace. The model includes radiative heating of the fiber mat and gases, fiber and gas energy balances and effects of fiber movement and residence time, gas flow and mixing of purge and carbonization off-gases, and fiber conversion due to fiber heating as it goes through the furnace. The model is cast as a steady state in order to model the conditions in continuous LT furnace during normal operation. The steady state formulation allows for computationally feasible simulations on average size computer clusters and workstations.

The developed model can be enhanced by implementing improved submodels for the above enumerated phenomena. However, the basic computational framework does not have to be changed. While the development of comprehensive coupled modeling capability has allowed the investigation of

influence of radiation and flow physics at a significantly higher fidelity, challenges remain in trying to understand the impact of processing parameters on the physical properties of fiber.

7. ACKNOWLEDGEMENTS

This research was supported by the High-Performance Computing for Manufacturing Project Program (HPC4Mfg), managed by the U.S. Department of Energy Advanced Manufacturing Office within the Energy Efficiency and Renewable Energy Office. This research used resources of the Compute and Data Environment for Science (CADES) at the Oak Ridge National Laboratory, which is supported by the Office of Science of the U.S. Department of Energy under Contract No. DE-AC0500OR22725. We greatly appreciate the Carbon Fiber Technology Facility (CFTF) supported by DOE's Advanced Manufacturing and Vehicle Technologies Offices within Energy Efficiency and Renewable Energy Office for providing experimental data for analysis.

8. REFERENCES

[1] Frank E, Steudle LM, Ingildeev D, Sporl JM, Buchmeiser MR. Carbon Fibers: Precursor Systems, Processing, Structure, and Properties. Angewandte Chemie-International Edition. 2014;53:5262-98.
[2] Jager H, Cherif C, Kirsten M, Behnisch T, Wolz DS, Bohm R, et al. Influence of processing parameters on the properties of carbon fibres - an overview. Materialwissenschaft Und Werkstofftechnik. 2016;47:1044-57.
[3] Morgan P. Carbon Fiber and their Composites: Taylor & Francis Group, LLC; 2005.
[4] Baukal CE. Heat transfer in industrial combustion: CRC Press LLC; 2010.
[5] Rahaman MSA, Ismail AF, Mustafa A. A review of heat treatment on polyacrylonitrile fiber. Polymer Degradation and Stability. 2007;92:1421-32.
[6] Jain MK, Abhiraman AS. Conversion of Acrylonitrile-Based Precursor Fibers to Carbon-Fibers. 1. A Review of the Physical and Morphological Aspects. Journal of Materials Science. 1987;22:278-300.
[7] Jain MK, Balasubramanian M, Desai P, Abhiraman AS. Conversion of Acrylonitrile-Based Precursors to Carbon-Fibers. 2. Precursor Morphology and Thermooxidative Stabilization. Journal of Materials Science. 1987;22:301-12.
[8] Balasubramanian M, Jain MK, Bhattacharya SK, Abhiraman AS. Conversion of Acrylonitrile-Based Precursors to Carbon-Fibers. 3. Thermooxidative Stabilization and Continuous, Low-Temperature Carbonization. Journal of Materials Science. 1987;22:3864-72.
[9] Hameed N, Sharp J, Nunna S, Creighton C, Magniez K, Jyotishkumar P, et al. Structural transformation of polyacrylonitrile fibers during stabilization and low temperature carbonization. Polymer Degradation and Stability. 2016;128:39-45.
[10] Lee T-S, Witting P. Computational Fluid Dynamics (CFD) analysis for Off-gas mixing and ventilation inside carbonization furnace during PAN-based carbon fiber manufacturing. Harper Int.; 2011.
[11] Lee T-S, Witting P. Kinetic Model of Stabilized PAN Fiber Mass Loss During Carbonization. Harper Int.; 2017.
[12] Lee T-S, Witting P. Advances in a Lumped Kinetic Model for Carbonization for Carbon Fiber Manufacturing. Harper Int.; 2018.
[13] Salim NV, Blight S, Creighton C, Nunna S, Atkiss S, Razal JM. The Role of Tension and Temperature for Efficient Carbonization of Polyacrylonitrile Fibers: Toward Low Cost Carbon Fibers. Industrial & Engineering Chemistry Research. 2018;57:4268-76.
[14] Pham HH, Lim YI, Cho CH, Bang YH. Hydrodynamics of low temperature carbonization furnace for production of polyacrilonitrile (PAN)-based carbon fiber. Chemical Engineering Research & Design. 2017;128:192-204.
[15] Convergent Science. CONVERGE CFD Software. https://convergecfd.com; 2018.

[16] Syamlal M, Rogers W, O`Brien TJ. MFIX Documentation: Theory Guide. Morgantow, WV: Morgantown Energy Technology Center; 1993. p. 54.
[17] Weller HG, Tabor G, Jasak H, Fureby C. A tensorial approach to computational continuum mechanics using object-oriented techniques. Computers in Physics. 1998;12:620-31.
[18] Coppalle A, Vervisch P. The Total Emissivities of High-Temperature Flames. Combustion and Flame. 1983;49:101-8.
[19] Smith TF, Shen ZF, Friedman JN. Evaluation of Coefficients for the Weighted Sum of Gray Gases Model. Journal of Heat Transfer-Transactions of the Asme. 1982;104:602-8.
[20] Tsai JS. Effect of Nitrogen Atmosphere on the Structure and Properties of a Pan-Based Carbon-Fiber. Textile Research Journal. 1994;64:772-4.
[21] Henrici-Olivé G, Olivé S. The chemistry of carbon fiber formation from polyacrylonitrile. Industrial Developments Advances in Polymer Science. 1983;51.
[22] Kaviany M. Essentials of Heat Transfer: Cambridge University Press; 2011.
[23] Oak Ridge National Laboratory. Carbon Fiber Technology Facility (CFTF). Oak Ridge, TN: Oak Ridge National Laboratory.
[24] Fiedler AK, Fitzer E, Rozploch F. PAN Pyrolysis Studied by Gas-Analysis and ESR-Analysis. Carbon. 1973;11:426-8.
[25] Ferziger JH, Perić M. Computational Methods for Fluid Dynamics. New York, USA: Springer; 1996.
[26] Cheng P. Two-Dimensional Radiating Gas Flow by a Moment Method. AIAA Journal. 1964;2:1662-4.
[27] Howell JR, Siegel R, Mengüç MP. Thermal Radiation Heat Transfer. 5th ed: CRC Press, Taylor & Francis Group; 2010.
[28] Patankar SV. Numerical Heat Transfer and Fluid Flow: Taylor & Francis; 1980.
[29] Casal JM, Porteiro J, Miguez JL, Vazquez A. New methodology for CFD three-dimensional simulation of a walking beam type reheating furnace in steady state. Applied Thermal Engineering. 2015;86:69-80.

9. APPENDIX

OpenFOAM utilities and workflow used in the simulations

#Start Preprocessing

runApplication blockMesh (This utility creates parametric meshes with grading along edges)

runApplication topoSet (This utility defines various regions with a label)

runApplication createPatch -overwrite (This utility creates patches out of selected boundary faces)

runApplication splitMeshRegions -cellZones -overwrite (This utility splits meshes into multiple regions)

runApplication changeDictionary (remove fields and introduce BCs in various zones created)

#Start Simulations

runApplication fiberFoam (new application created for this project based on reactingFoam)

#Start Postprocessing

paraFoam -touchAll (creating files for paraview post-processing)